



Separation of heavy rare-earth elements by non-aqueous solvent extraction: Flowsheet development and mixer-settler tests

Brecht Dewulf, Sofía Riaño, Koen Binnemans*

KU Leuven, Department of Chemistry, Celestijnenlaan 200F, P.O. box 2404, Leuven B-3001, Belgium

ARTICLE INFO

Keywords:

Counter-current liquid-liquid extraction
Lanthanides
Process development
Solvometallurgy

ABSTRACT

The separation of rare-earth elements (REEs) is considered one of the most challenging processes in solvent extraction. In recent years, non-aqueous solvent extraction, a unit operation within solvometallurgy, has stepped into the limelight as one of the promising techniques for efficient REEs separation. In this paper, a rare-earth hydroxide concentrate, originating from mining waste and containing mainly heavy rare-earth elements (HREEs), was redissolved in ethylene glycol + 10 vol% water, 0.43 mol L⁻¹ HCl and 0.8 mol L⁻¹ NaCl. Based on batch experiments, a conceptual flowsheet was proposed for the separation of the HREEs into 2 groups: a thulium group (Tm, Yb and Lu) and a dysprosium group (Dy, Ho, Er and Y). Continuous solvent extraction tests in lab-scale mixer-settlers were performed to confirm the technical feasibility of the developed system, as well as to identify and resolve possible bottleneck points. Eventually, using only 16 stages of lab-scale mixer-settlers, the purity of the thulium group and dysprosium group elements, originally 34% and 54%, respectively, reached 99.8% and 98.7%, respectively. Further optimization remains necessary for the separation and purification into highly pure single REEs.

1. Introduction

Rare-earth elements (REEs) comprise the 15 lanthanides, Y and Sc, and are subdivided by industry into two major groups: the light rare-earth elements (LREEs) from La up to Eu and the heavy rare-earth elements (HREEs) from Gd up to Lu [1]. Y mostly behaves as a HREE, while the chemical behaviour of Sc often deviates from the rest of the REEs, despite their similar electronic structure. While the economic importance of the LREEs is primarily dominated by Nd and Pr, with Nd-Fe-B permanent magnets being the most important application [2,3], HREEs are mainly used in niche applications of strategic importance, such in laser crystals, optical amplifiers, high-tech alloys and ceramics, and medical applications [4,5]. While these applications only contain small quantities of high-purity HREEs, the strategic importance of the HREEs in terms of national defence and the sharp growth in demand combined with limited production has led to increased research awareness [1]. While increased production of primary resources might alleviate shortages in the short term, the recovery of HREEs from secondary resources will play a significant role on a longer-term basis. This includes recycling of industrial scraps and end-of-life products, as well as recovery of REEs from mining wastes [3,6].

Efficient separation of HREEs into individual elements or groups is key for their use in different applications. While various new solid-liquid separation approaches have been investigated in recent years, such as functionalized resin systems [7,8] and functionalized membrane systems [9,10], the main industrial focus remains on liquid-liquid extraction [11,12]. The current state-of-the-art used in Chinese HREE separation plants makes use of saponified P507, i.e. 2-ethylhexyl phosphoric acid mono-2-ethylhexyl ester, extracting the HREEs from HCl solution [13,14]. Major drawbacks of this system are the large consumption of acids and bases for pH control, the emulsion formation due to Fe, Al or Si impurities or upon exceeding the maximum extraction capacity of the acidic extractant, and the large quantities of highly acidic stripping solutions needed for a complete stripping of the HREEs [13–16]. Recently, a modification in the form of the synergistic system Cyanex 272 [bis(2,4,4-trimethylpentyl)phosphinic acid] + P507 was proposed [17]. The main advantages of this system were the increased separation factors between the HREEs and the reduction of scrubbing and stripping solution acidity. However, also a reduction in extraction capacity was observed. Improving stripping efficiency at lower acidity was also obtained by addition of 2-ethylhexanol (isooctanol) to P507 [17,18]. Besides adjusting the composition of the organic phase

* Corresponding author.

E-mail address: Koen.Binnemans@kuleuven.be (K. Binnemans).

containing extractants and additives, researchers also investigated modifications of the conventional flowsheet design. The type of process known as the “*hyperlink process*”, also often called fuzzy(-link) separation, is frequently used in HREE separation in combination with P507 or P507 + Cyanex 272, and focuses on the separation of the least- and most-extractable elements, providing a rough separation, i.e. ABC are separated in AB and BC, followed by a next, linked separation into A, B and C [13,19,20]. The main advantages are the reduction in the use of saponification reagents and the reduction in the number of stages needed for the separation.

Until recently, research mostly focused on the optimization of the flowsheet design or on optimizing the organic phase composition [12,20–22]. In contrast, *non-aqueous solvent extraction* (NASX), a unit operation within solvometallurgy, focusses on replacing the aqueous phase largely by a non-aqueous phase [23]. This non-aqueous phase can be a polar molecular organic solvent or an ionic solvent (such as molten inorganic salts, molten hydrates, and ionic liquids) [24]. As NASX systems often have two organic phases, a distinction needs to be made between the more polar (MP) phase containing the original metals mixture to be extracted, and the less polar (LP) phase, containing the extractant(s), diluent and sometimes a modifier. The origin of the research presented in this paper can be traced back to a publication by Batchu et al., mentioning for the first time the remarkable separation of REEs from ethylene glycol (EG) nitrate and chloride media, using Cyanex 923 [25,26]. In nitrate media, extraction of LREEs from EG is less efficient than extraction from water, while extraction of HREEs from EG is more efficient than extraction from water, resulting in large separation factors for the middle rare-earth elements (MREEs) in particular. In chloride media, REEs are almost not extracted from aqueous solutions, while ethylene glycol solutions increase extraction efficiencies for all REEs significantly, which is more pronounced for the HREEs, hence resulting in enhanced separation factors between different HREEs. Research on specific applications for these systems resulted in flowsheets for the separation of Y/Eu [27], Nd/Dy [28], the separation of REEs from transition metals [29,30], as well as the separation of In/Zn [31].

While there are already many works on the separation of two or more REEs from a simple matrix, only a few researchers have studied the separation of a mixture of REE ions, in complex mixtures originating from industrial concentrates. The present paper focusses on NASX for the separation of a broad range of REEs and impurities, present in widely different concentrations, starting from an industrial rare-earth hydroxide concentrate originating from sulfidic mining waste. The processing of this mining waste to obtain the HREE concentrate was a part of the Horizon 2020 NEMO project [32]. We propose a conceptual flowsheet for HREE separation, based on lab-scale single contact experiments. To validate the developed process and identify possible bottlenecks, the flowsheet was tested in continuous counter-current mode with mini-pilot mixer-settlers. The results from these tests and the challenges encountered are discussed in detail.

2. Experimental

2.1. Products

Ethylene glycol (99.5%), petroleum ether (kerosene, boiling range 180–280 °C, flash point 83 °C), *p*-cymene ($\geq 99\%$), H_2O_2 (99.9%), and Aliquat 336 TG were obtained from Acros Organics (Geel, Belgium). Hydrochloric acid (37 wt%), toluene ($\geq 99.8\%$), NaCl ($\geq 99.5\%$), NaOH (99.3%) and MgO (98%) were supplied by Fisher Scientific (Geel, Belgium). Cyanex 923, a mixture of trialkyl phosphine oxides, with C_6 and C_8 chains, was purchased from Solvay (Niagara Falls, Canada). Nitric acid, 1-butanol and the ICP standards (1000 ppm, in 3–5 wt% HNO_3) were obtained from Chem-Lab (Zedelgem, Belgium). The ICP standards of the following elements were used: Al, Ca, Fe, Mg, Sc, Mn, Ni, Zn, Y, Dy, Ho, Er, Tm, Yb, Lu. LiCl was supplied by Carl Roth

(Karlsruhe, Germany). L-ascorbic acid (99%), $\text{Al}(\text{OH})_3$ (hydrate, 50–57.5% Al_2O_3 basis), Fe_2O_3 ($\geq 99\%$), MnO (99%), NiO (99%) and ZnO (99%) were purchased from Sigma-Aldrich (Steinheim, Germany). Y_2O_3 (99.9%) was obtained from REacton (Kandel, Germany) Dy_2O_3 (99.9%) and Er_2O_3 (99.9%) were supplied by Strem Chemicals (Newburyport, USA). Tm_2O_3 (99.99%), Yb_2O_3 (99.9%), and Lu_2O_3 (99.99%) were purchased from Treibacher Industries AG (Althofen, Austria). Water was always of ultrapure quality (less than $0.055 \mu\text{S cm}^{-1}$ at 298.15 K) using a Merck Millipore Milli-Q Reference A + system. All chemicals were used as received, without any further purification.

2.2. Elemental analysis

The elemental composition of aqueous and non-aqueous solutions was determined by ICP-OES (Perkin-Elmer Avio 500). All samples were measured in triplicate. The calibration curves were obtained by measurement of standard solutions spanning the expected sample concentration range. Scandium (5 mg L^{-1}) was used as internal standard. Quality control checks were carried out after measuring the calibration curve and after every 10 samples. For aqueous and ethylene glycol solutions, the spectrometer was equipped with a GemCone High Solids nebulizer, baffled cyclonic spray chamber, 2.0 mm inner diameter alumina injector and PerkinElmer Hybrid XLT torch. These types of samples (including quality controls and calibration standards) were diluted using a 2 wt% HNO_3 solution to reach the desired concentration range. For solutions of petroleum ether containing Cyanex 923 and extracted metals, the spectrometer was equipped with a Meinhard Low-Flow nebulizer, baffled cyclonic spray chamber, 1.2 mm inner diameter alumina injector and PerkinElmer Hybrid XLT torch. These type of samples (including quality controls and calibration standards) were diluted using 1-butanol to reach the desired concentration range. Table S1 in Supporting Information (SI) gives an overview of the measured lines used for calculation of the results, for each element. Only results obtained by measuring in axial mode were used for calculations.

2.3. Dissolution of rare-earth hydroxide concentrate

The information on the elemental composition of the industrial rare-earth hydroxide concentrate and the synthetic rare-earth hydroxide concentrate can be found in SI. Only the latter was used for dissolution experiments. These experiments are performed on a reactor platform constructed by HiTec Zang (Germany, Figure S1). The jacketed reactor used in this experiment had a volume of 1 L. The Heidolph Hei-TORQUE Precision 200 stirrer was equipped with an anchor shaped impeller. During the experiment, the dissolution was tracked by sampling (about 0.5 mL) at regular time intervals. The aliquots were filtered using Chromafil PET syringe filters ($0.45 \mu\text{m}$ pore size), before sample preparation for elemental analysis by ICP-OES.

2.4. Lab-scale solvent extraction procedure

The feed solutions (MP phase) used for these experiments consisted of ethylene glycol, 10 vol% water (unless stated differently), the impurities and REEs to be separated, and either LiCl or NaCl as a salting-out agent. The preparation of the MP phase is discussed in SI. The extractant, Cyanex 923, is dissolved in petroleum ether (kerosene), and will be indicated as less polar (LP) phase. The MP and LP phase are shaken for a minimum of 15 min at 300 rpm using a wrist-action shaker at room temperature ($21 \pm 1 \text{ }^\circ\text{C}$). A contact time of 15 min was sufficient, as the time to reach chemical equilibrium is less than 5 min. Moreover, the viscosity of the MP phase at $25 \text{ }^\circ\text{C}$ was 19.3 mPa s (density 1.38 g mL^{-1}), which is sufficiently low for good mass transfer rates, while phase disengagement was slower (average settling rate 0.6 mm s^{-1}) compared to aqueous systems. The phase ratio was generally 1:1 (3 mL : 3 mL) and 10 mL glass vials were used, except during lab-scale tests with varying phase ratios, to construct a McCabe-Thiele diagram, where the total

volume was 12 mL and 20 mL glass vials were used.

After extraction, the sample vials were centrifuged at 3000 rpm for 2 min, to accelerate phase separation. The MP phase was sampled for elemental analysis using the ICP-OES and appropriately diluted using a 2 wt% HNO₃ solution. The LP phase was only sampled in case of a lab-scale scrubbing or stripping experiment, or in case of mixer-settler pilot tests (*vide infra*). From the results, the (*concentration*) *distribution ratio* (D_c), the *extraction factor* (D_m), also called *mass distribution ratio*, and the *percentage extraction* (%E) can be calculated as defined by equation (1) – (3).

$$D_c = \frac{c_i - c_{MP}}{c_{MP}} \quad (1)$$

$$D_m = D_c \cdot \frac{V_{LP}}{V_{MP}} \quad (2)$$

$$\%E = \frac{D_c}{D_c + V_{MP}/V_{LP}} \cdot 100 \quad (3)$$

Here, c_i is the metal concentration of the MP phase before the extraction, c_{MP} and c_{LP} are the metal concentrations in the MP and LP phase, respectively, after extraction. V_{MP} and V_{LP} are the volumes of the MP and LP phase, respectively. The *separation factor* (α_{AB}), defined by equation (4), is the quotient of the distribution ratio of a metal A over that of metal B, with $\alpha_{AB} > 1$.

$$\alpha_{AB} = \frac{D_{c,A}}{D_{c,B}} \quad (4)$$

2.5. Mixer-settler procedure

The continuous, counter-current mixer-settler experiments were performed in a SX Kinetics lab-scale pilot (Ontario, Canada) consisting of borosilicate glass mixer and settling chambers, as shown in Figure S2. The mixer has a volume of 270 mL, while the column-shaped settler has a volume of 1050 mL and a settling area of about 35 cm². The stirrers (Caframo model BDC 250) were set at 1000 rpm during all experiments. Cole-Parmer Masterflex L/S peristaltic pumps were used, in combination with Masterflex L/S Easy-Load pump heads. During operation, once hydraulic equilibrium was attained, samples of the MP and LP phase were taken every hour from each stage, to track the concentration changes and check for chemical equilibrium. An overview of the operating conditions of each mixer-settler experiment can be found in Table S4.

3. Results and discussion

3.1. Dissolution of rare-earth hydroxide concentrate

The main goal of this paper is to develop a non-aqueous process for the separation of REEs, that is competitive with conventional aqueous solvent extraction systems, and to test this process in continuous mode. For this, a MP feed solution consisting of ethylene glycol + 0.8 mol L⁻¹ NaCl was prepared by dissolving a synthetic rare-earth hydroxide concentrate (for preparation and concentrations: see SI, Table S3). The target concentration for REE content in the MP phase was 10 g L⁻¹. For the optimization of the dissolution parameters, various HCl concentrations, water concentrations and temperatures were tested. As to the HCl concentration, it was opted to limit the excess concentration of HCl, as the neutral extractant Cyanex 923 is known to extract mineral acids, causing problems in the downstream solvent extraction process [33]. It was determined that a maximum of 0.1 mol L⁻¹ HCl can be allowed in the MP feed solution, as this concentration has negligible effects on the extraction behaviour. The concentration of water on the other hand has a profound effect on the dissolution rate and, more importantly, on the downstream extraction behaviour as well. Lab-scale extraction experiments have shown that the optimal water concentration is 10 vol% (*vide*

infra). The influence of temperature was studied in larger-scale experiments using a jacketed leaching reactor (1 L). Based on the results shown in Figure S3, it became evident that dissolution at room temperature was incomplete, and elevated temperatures were needed to complete the dissolution within a reasonable time frame. One must be careful, however, as elevated temperatures promote the potential formation of trace amounts of 2-chloroethanol [34]. Therefore, it is advised to use lower temperatures and appropriate stirring speeds that allow efficient mixing. Dissolution at abovementioned conditions did not result in any selectivity, as the metal impurities in the concentrate are quantitatively dissolved as well at the optimal conditions for REEs dissolution, except for Al (about 85–90% dissolved). Eventually, a MP feed consisting of ethylene glycol + 10 vol% water and 0.8 mol L⁻¹ NaCl was obtained after the dissolution, with average metal concentrations as shown in Table 1. A sufficient volume of this MP feed was prepared, to be used in batch-scale and in continuous counter-current experiments. In conventional REE separation processes, the REE concentration is about 1–1.5 mol L⁻¹, approximately 10–20 times higher than in the present NASX pilot process, i.e. 10 g L⁻¹ or about 0.07 mol L⁻¹. The REE concentration in ethylene glycol + 10 vol% water is limited by the maximum concentration of the aqueous HCl solution (37 wt%) added to ethylene glycol. Hence, the maximum REE concentration when dissolving REE hydroxides is 60 g L⁻¹ (about 0.4 mol L⁻¹). In contrast, the solubility of REEs as chloride salts in EG is much higher, for instance 1.6 mol L⁻¹ for NdCl₃ [35]. The extraction behaviour in the present lab-scale pilot is expected to be representative for the industrial scale, though further optimisation of distribution ratios and separation factors might be necessary for higher REE concentrations.

3.2. Lab-scale solvent extraction optimization

The extractant used in the less polar (LP) phase is the neutral extractant Cyanex 923, a commercial mixture of trialkyl phosphine oxides, with C₆ and C₈ chains [36]. It has the advantage over trioctylphosphine oxide (TOPO) that it is a liquid at room temperature and it is a stronger extractant than tri-*n*-butyl phosphate (TBP). The diluent is petroleum ether, also known as kerosene, having a boiling range of 180–280 °C and a flashpoint of 82 °C, which is sufficiently high for safe operation at ambient temperature. The salting-out agent concentration (LiCl) and water content of the MP phase were optimized (Fig. 1). The metal concentrations in these feed solutions are given in Table 1. The general trend for the extraction efficiency of the different REEs follows the increasing order: Dy < Y ≈ Ho < Er < Tm < Yb ≈ Lu. The largest separation factors can be found for the Er – Tm separation. The LiCl concentration clearly increases the percentage extraction, as it promotes the formation of REE – chloride contact-ion pairs and reduces the activity of water and ethylene glycol. Water has an overall negative impact on extraction efficiency, primarily caused by the strong hydration of the HREEs and the lack of ion pair formation [24,37], which is particularly pronounced at lower LiCl concentrations and for the lighter HREEs. At 10 vol% water and 0.8 mol L⁻¹ LiCl, the separation factor was 3, which is equal to or even slightly higher than the separation factors reported in previous studies [7,13,38–40], for instance $\alpha_{Er,Tm} = 1.1$ –2.5, depending

Table 1
Average metal concentrations in MP phase.

Impurities		Rare-earth elements	
element	Concentration (mg L ⁻¹)	element	Concentration (mg L ⁻¹)
Al	297 (±3)	Dy	75 (±2)
Ca	207 (±7)	Ho	46 (±1)
Fe	34 (±1)	Er	400 (±5)
Mg	23 (±1)	Tm	252 (±3)
Mn	166 (±2)	Yb	2595 (±37)
Ni	49 (±1)	Lu	536 (±8)
Zn	142 (±3)	Y	5135 (±113)

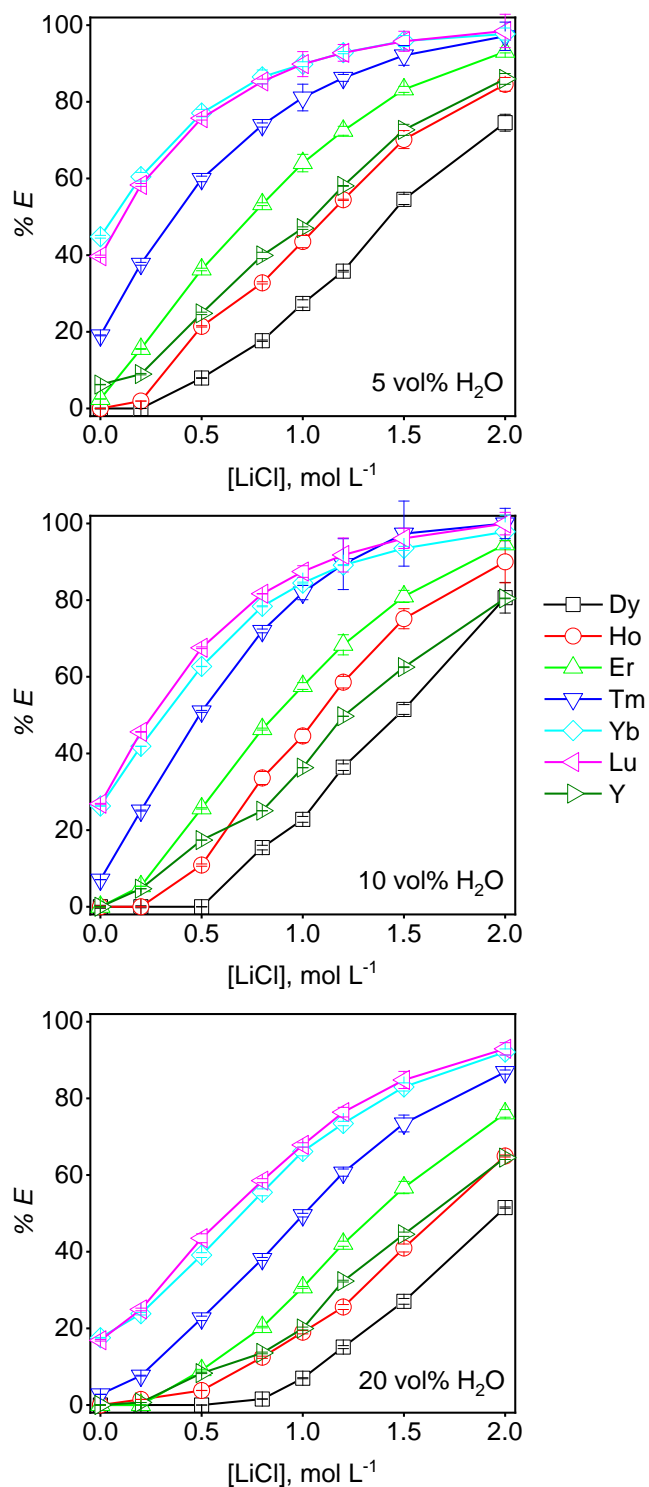


Fig. 1. Effect of water concentration and LiCl concentration on the extraction of REEs. Conditions: MP phase = ethylene glycol + varying water and LiCl concentrations, average initial metals concentration shown in Table 1, LP phase = 1 mol L⁻¹ Cyanex 923 in petroleum ether. Phase ratio MP:LP = 1:1, room temperature.

on the conditions, for the conventionally used P507-kerosene-HCl system [14,41]. The major advantage of this system, however, is the possibility to use a solvating extractant for REE separation, which involves negligible consumption of acids and bases compared to the conventionally used acidic extractants. Moreover, stripping of REEs from Cyanex 923 is much easier, reducing the number of stages significantly.

The extraction system does not require a modifier, making the system simpler and less expensive. The extraction factor, as defined in Equation (2), is a useful tool for determining the position in which the REE series can be separated into one or more groups [42]. The two elements which can be separated from each other, to establish REE group separation, are defined as the lower key and upper key elements, the former having D_m less than 1 and the latter $D_m > 1$. In our case, Er has $D_m = 0.86$ and Tm has $D_m = 2.56$. As to the transition metals (Figure S4) it can be seen that Zn and Fe are extracted quantitatively, while Mg and Ni are not extracted (within the errors on the analytical measurements). Extraction of Al, Ca and Mn is strongly dependent on the water concentration. The percentage extraction of Al, Ca and Mn is reduced from 80%, 15% and 40%, respectively, at 5 vol% water and 1 mol L⁻¹ LiCl, to 20%, 0% and 20%, respectively, at 20 vol% water and 1 mol L⁻¹ LiCl.

To make the process more economically feasible, it was attempted to replace LiCl by NaCl as salting-out agent. To this end, the influence of the Cyanex 923 concentration was studied by extraction from a MP phase containing either 0.8 mol L⁻¹ LiCl or NaCl (Fig. 2 and Figure S5). In both cases, the same order of extraction and very similar extraction efficiencies were obtained. Also, it was observed that the optimum Cyanex 923 concentration for REE separation would be 1 mol L⁻¹, reaching the highest Er/Tm separation factor, i.e. 3. A complete overview of the REE separation factors can be found in Table S5. For the transition metals, it was observed that extraction of Zn and Fe were already 88% and 100%, respectively, even at 0.2 mol L⁻¹ Cyanex 923, while extraction of other impurities was negligible. To avoid REE losses, 0.1 mol L⁻¹ was considered to be optimal for the removal of Zn and Fe

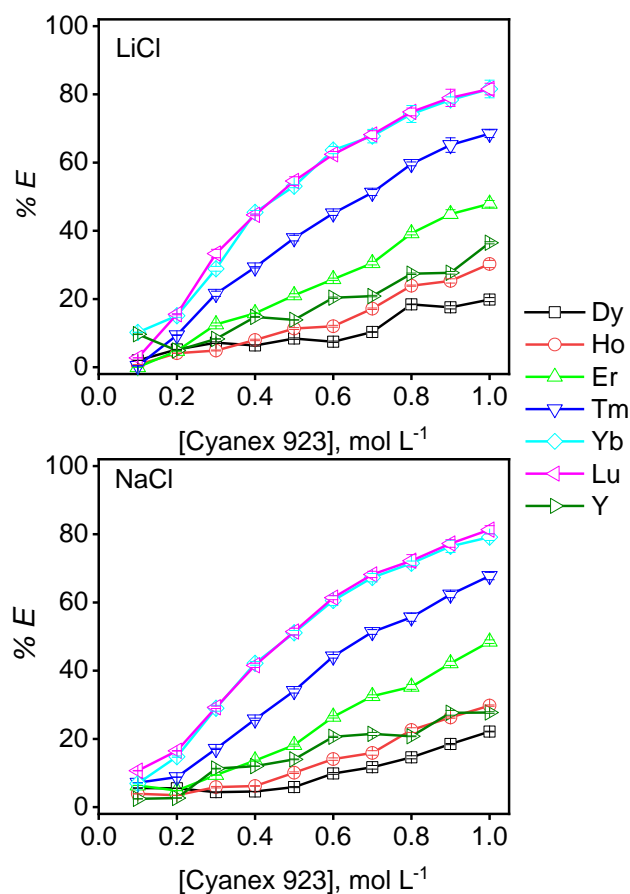


Fig. 2. Comparison of LiCl (top) and NaCl (bottom) as salting-out agent at varying Cyanex 923 concentrations. Conditions: MP phase = ethylene glycol + 10 vol% water, [NaCl] = [LiCl] = 0.8 mol L⁻¹, average initial metals concentration shown in Table 1, LP phase = 0.1–1 mol L⁻¹ Cyanex 923 in petroleum ether. Phase ratio MP:LP = 1:1, room temperature.

was investigated. The total impurity content is about 0.9 g L^{-1} (Table 1). Therefore, it was opted to introduce an extraction step using Cyanex 923, to remove Zn and Fe from the feed solution (extraction SX1), as these are the most problematic impurities due to their high affinity for Cyanex 923. The optimal concentration of extractant was 0.1 mol L^{-1} Cyanex 923 diluted in petroleum ether, which avoided the loss of REEs while extracting most of Zn and Fe. A McCabe-Thiele diagram (Figure S6 a–b) was constructed based on the distribution isotherm for Zn and Fe, indicating the need for 3 stages to completely remove both elements, at a phase ratio of 2:1. As the mini-pilot mixer-settler used in this work is designed to handle phase ratios between 1.5:1 and 1:1.5, it was chosen to work with a phase ratio of MP:LP = 1.5:1, and 3 stages.

As to the mixer-settler experiment, the flow rates used in this piloting experiment were 1.08 L h^{-1} and 0.72 L h^{-1} for the MP and LP phase, respectively. The mixer-settler setup originally used 3 stages, yet as the percentage of Fe extracted at equilibrium was considered low, a fourth stage was added. Chemical equilibrium was attained in less than 8 h: metal concentrations remained constant, with only minor variations from one hour to the other. Neither third phase formation, nor precipitation were noticed during the entire process. Limited entrainment of the LP phase into the MP phase was visible. The concentration profile of Zn and Fe in the MP phase is shown in Fig. 4, while other concentrations are given in Table S6. Almost complete extraction of Zn (97%) and Fe (93%) was obtained, while the loss of REE was limited: there was only a measurable loss for Lu, i.e. 2% co-extraction.

3.5. Separation of Tm-group from Dy-group elements

In a next step, Tm-group elements (Tm, Yb, Lu) were separated from Dy-group elements (Dy, Y, Ho, Er), through extraction of the former (extraction SX2). McCabe-Thiele analysis on the extraction isotherm of Tm (Figure S6 c) revealed that quantitative extraction of this element requires a volume ratio of MP:LP = 1.25:1 and would require 6 counter-current stages. To further upconcentrate the metals in the LP, the volume ratio was chosen MP:LP = 1.5:1, and it was opted to test 7 stages instead, to assure complete extraction. The flow rates used in this piloting experiment were 2.48 L h^{-1} and 1.65 L h^{-1} for the MP and LP phase, respectively. Chemical equilibrium was attained within 4 h of the start of the experiment, with metal concentrations in both MP and LP phases remaining constant afterwards. Neither third phase formation, nor precipitation were noticed during the entire process. However, the presence of an emulsion at the interphase in the settlers was

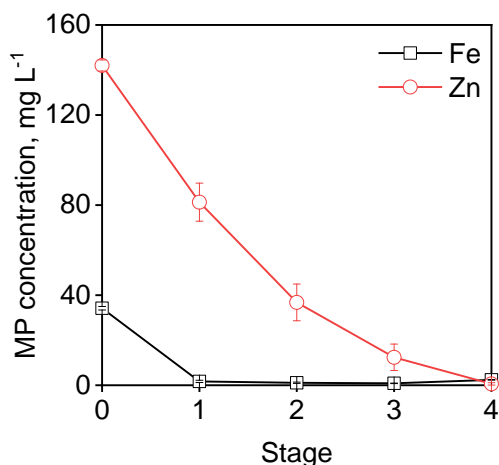


Fig. 4. Concentration profile of Fe and Zn in the MP phase during extraction (SX1). Conditions: MP phase (enters at stage 1): ethylene glycol + 10 vol% water, $[\text{NaCl}] = 0.8 \text{ mol L}^{-1}$, initial metal concentrations shown in Table 1, LP phase (enters at stage 4): 0.1 mol L^{-1} Cyanex 923 in petroleum ether. Flow ratio MP:LP = 1.5:1, retention $t = 9 \text{ min}$ per mixer, room temperature.

troublesome, as it threatened adequate phase disengagement in the settler. When a large amount of emulsion was present, the problem was tackled by reducing the stirring speed and the flows until the emulsion broke. Given the rather slow disengagement rates observed in NASX systems (Table S4), the mixer-settler design could be optimized for non-aqueous systems by, for instance, enlarging the settling tank and providing coalescence plates. As to the extraction results, good extraction efficiencies for Tm, Yb and Lu were reached, i.e. 95.4%, 99.4% and 99.4%, respectively. The concentration profiles of the REEs are shown in Fig. 5 and detailed extraction results are shown in Table S6. Coextraction of Er (70.5%, 274 mg L^{-1}) as well as of Y (37.7%, 1743 mg L^{-1}) was considerable.

To solve the issue of coextraction, scrubbing of Dy, Ho, Er, Y and metal impurities from the loaded LP phase (scrubbing SX3) was studied using a MP scrub solution consisting of ethylene glycol + 10 vol% water and 0.8 mol L^{-1} NaCl. Based on the distribution isotherm (Figure S6 d) for Er scrubbing, a 7-stage scrubbing process at MP:LP = 1.5:1 was chosen to be optimal. The flow rates used in this mini-piloting experiment were 2.48 L h^{-1} and 1.65 L h^{-1} for the MP and LP phase, respectively. Chemical equilibrium in all stages was attained within 5 h of continuous operation after the start of the experiment, with metal concentrations in both MP and LP phases remaining constant afterwards. Neither third phase formation, nor precipitation were noticed during the entire process. Moreover, emulsion formation was limited, and thus less problematic than experiment SX2. An overview of the mixer-settler extraction results can be found in Table S6 and the concentration profiles of the REEs in both MP and LP phases can be found in Fig. 6. The scrubbing step removed nearly all of the coextracted impurities, at the cost of a loss of Tm (78%), Yb (44%) and Lu (42%). However, the MP raffinate phase can be recycled to the previous extraction step (SX2) to replace a part of the feed phase, minimizing this loss.

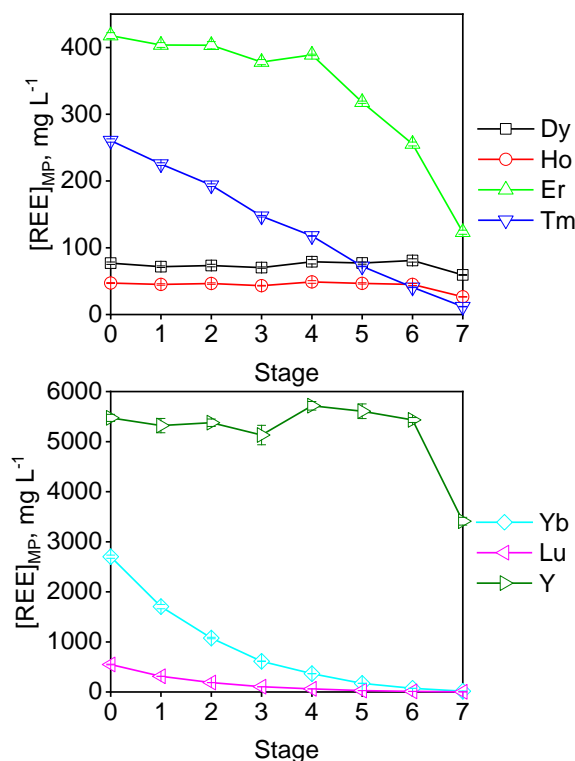


Fig. 5. REE concentration profile, subdivided according to concentration for clarity, in the MP phase during extraction (SX2). Conditions: MP phase (enters at stage 1): ethylene glycol + 10 vol% water, $[\text{NaCl}] = 0.8 \text{ mol L}^{-1}$, initial metal concentrations shown in Table S6 (SX1), LP phase (enters at stage 7): 1 mol L^{-1} Cyanex 923 in petroleum ether. MP:LP ratio = 1.5:1, retention $t = 4 \text{ min}$ per mixer, room temperature.

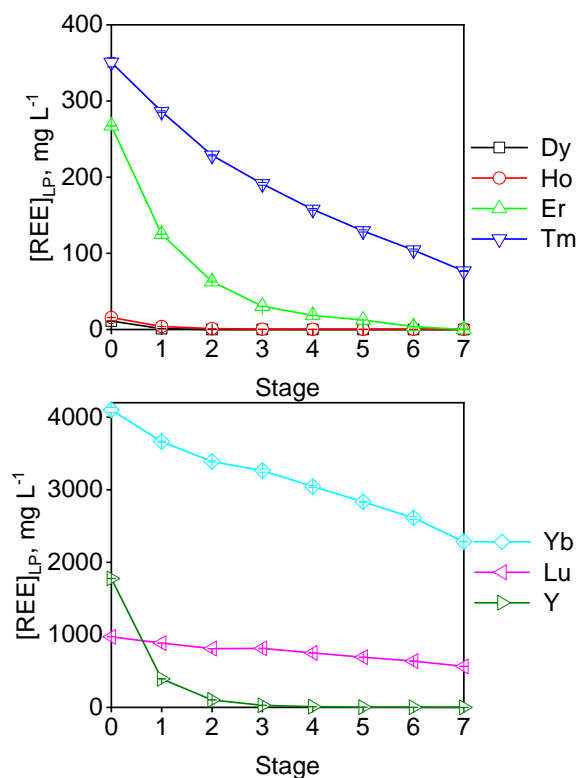


Fig. 6. Concentration profile of the REE, subdivided according to concentration for clarity, in the LP phase during scrubbing (SX3). Conditions: MP phase (enters at stage 7): ethylene glycol + 10 vol% water, $[\text{NaCl}] = 0.8 \text{ mol L}^{-1}$, LP phase (enters at stage 1): 1 mol L^{-1} Cyanex 923 in petroleum ether, initial metal concentrations shown in Table S6 (SX2). Flow ratio MP:LP = 1.5:1, retention $t = 4 \text{ min}$ per mixer, room temperature.

3.6. Extraction and purification of Er

In addition to group separation of the HREEs, it was attempted to separate and purify Er from the Dy-group elements (extraction SX4). Similar to the extraction of the Tm-group elements, a LP phase containing 1 mol L^{-1} C923 diluted in petroleum ether was used. The extraction factors during lab-scale tests were 0.64 and 1.18 for Ho and Er, respectively, at a phase ratio of MP:LP = 1:1, indicating the possibility of separation. A McCabe-Thiele diagram constructed using the distribution isotherm of Er (Figure S6 e) revealed that 4 stages would be necessary at MP:LP = 1:1.5. The mixer-settler experiment (extraction SX4) was performed using the parameters summarized in Table S4. Although the technical execution went smoothly, the extraction results (Table S6) were not satisfactory. While Er was extracted almost quantitatively (98.5%) after 4 stages, the coextraction of Ho (92%, loaded LP concentration 17 mg L^{-1}), and especially of Y (90%, loaded LP concentration 2147 mg L^{-1}) were high. The concentration profile throughout the 4 stages can be found in Figure S7. To remove Ho and Y from the loaded LP phase, scrubbing was tested in batch experiments using a scrub solution containing ethylene glycol + 10 vol% water and various NaCl concentrations as the MP phase. Eventually, a NaCl concentration of 0.4 mol L^{-1} was chosen to be optimal, as lower concentrations caused Er to be lost almost completely to the MP phase, while higher concentrations did not manage to lower Ho and Y concentrations in the LP phase substantially. However, the McCabe-Thiele diagram constructed for Y (Figure S6 f) indicated that Y cannot be removed completely from the LP phase due to the so-called ‘pinching effect’, i.e. the operating line and distribution isotherm are overlapping. To verify these findings, a 3-stage mixer-settler experiment (scrubbing SX5) was performed using the above mentioned optimized MP scrub feed. As

expected, only about 90.7% of Y was scrubbed, leaving about 250 mg L^{-1} in the LP phase (Table S6). The concentration of Er left in the LP phase is low, around 20 mg L^{-1} . To make this process step technically and economically relevant, further optimization of the flows and concentrations is required. The concentration profile for the 3 scrubbing stages can be found in Figure S8.

3.7. Extraction of Dy-group elements

The MP phase raffinate after the extraction of Er still contained high concentrations of REEs, primarily Y (Table S6). Precipitation of REEs by adding oxalic acid directly to the ethylene glycol MP phase was not possible, given the high solubility of rare-earth oxalates in this solvent. With regard to technical feasibility on the lab-scale mixer-settlers, it was opted to extract the REEs using a higher concentration of Cyanex 923 and to maintain a higher MP:LP ratio, in order to increase extraction efficiency and to lower the number of stages needed. However, increasing the concentration of Cyanex 923 caused volume changes, which were previously not observed at a concentration of 1 mol L^{-1} . Mutual solubility studies performed on the latter system have indeed shown that the solubility of ethylene glycol in the LP phase is limited [26]. The volume change observed when increasing Cyanex 923 concentration is caused by the increase in polarity of the LP phase, causing increased ethylene glycol solubility. At 2 mol L^{-1} Cyanex 923, the LP phase volume increased about 12% (MP:LP changed from $5 \text{ mL} : 5 \text{ mL}$ to $4.4 \text{ mL} : 5.6 \text{ mL}$) after contact with a MP phase containing ethylene glycol + 10 vol% water and 0.8 mol L^{-1} NaCl. Therefore the MP was presaturated by equilibration with a solution of ethylene glycol + 10 vol% water and 0.8 mol L^{-1} NaCl in mixer-settlers prior to the solvent extraction experiments. Eventually, the extraction of the REEs from the abovementioned raffinate (extraction experiment code SX6) was performed using the presaturated LP phase (2 mol L^{-1} Cyanex 923) by a 2-stage mixer-settler setup at a phase ratio MP:LP of 1:1, as determined by the McCabe-Thiele diagram based on Dy and Y extraction isotherms (Figure S6 g–h). The flow rates were 1.26 L h^{-1} for both the MP and LP phases. Chemical equilibrium was attained within 4 h after the start of the experiment, with metal concentrations in both MP and LP phases remaining constant afterwards. Neither third phase formation, nor precipitation were noticed during the entire process. Due to relatively slow phase disengagement (0.6 mm s^{-1} for MP phase continuous, 0.1 mm s^{-1} for LP phase continuous), the formation of large dispersion bands was inevitable, but the phases could still be separated in the settler. An overview of the results can be found in Table S6 and the concentration profiles of the REEs in both MP and LP phases can be found in Fig. 7. Quantitative extraction was obtained for all REEs. The impurity metals did not extract quantitatively, and Ni did not extract at all.

3.8. Stripping

Precipitation stripping using aqueous oxalic acid solutions was used to recover the rare-earth values from the different loaded LP phases, and also allows to recycle the latter. The loaded LP phases that were treated were obtained after (1) the scrubbing of coextracted Dy-group elements, (2) the scrubbing of Dy, Ho and Y from the Er-rich LP phase, (3) the extraction of left-over Dy-group elements. The batch experiments were conducted by contacting the LP phases with aqueous solutions in a ratio of MP:LP = 1:1, with the aqueous phase containing 1, 1.2, 1.4, 1.6, 1.8 or 2 times the stoichiometric amount of oxalic acid needed to precipitate all metals. It was found that 2 times the stoichiometric amount was optimal, as it allowed to remove the HREEs quantitatively, while reducing the loss of HREEs to the aqueous phase due to the partial solubility of HREE oxalates. Lowering the MP:LP ratio while maintaining the oxalic acid stoichiometry negatively impacted the stripping efficiency. To enhance the phase disengagement of the two phases after stripping, it was opted to work at a temperature of $50 \text{ }^\circ\text{C}$. The stripping was upscaled (MP:LP =

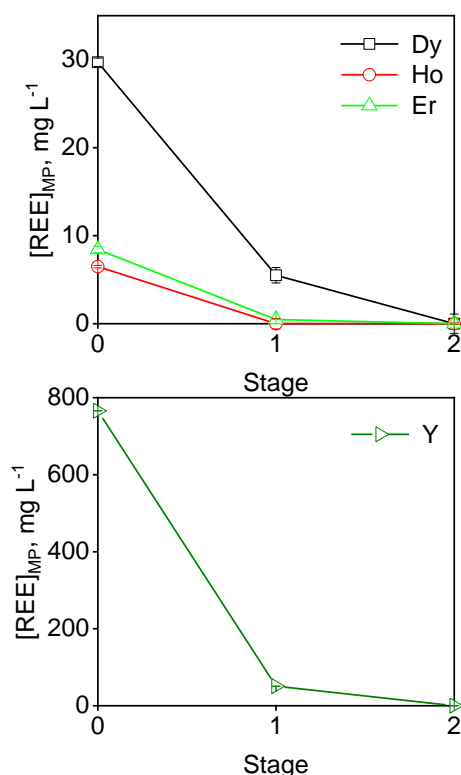


Fig. 7. Concentration profile of the REEs, subdivided according to concentration for clarity, in the MP phase during extraction (SX6). Conditions: MP phase (enters at stage 2): ethylene glycol + 10 vol% water, $[\text{NaCl}] = 0.4 \text{ mol L}^{-1}$, initial metal concentrations shown in Table S6, LP phase (enters at stage 1): 2 mol L^{-1} Cyanex 923 in petroleum ether. Flow ratio MP:LP = 1:1, retention $t = 6 \text{ min}$ per mixer, room temperature.

1 L: 1 L) for the three abovementioned loaded LP phases, using the optimized parameters. The results, shown in Table S7, are in agreement with the lab-scale observations, and show quantitative stripping of the REEs, with limited losses to the MP phase. The coextracted Al did not precipitate quantitatively, yet largely reported to the MP phase instead. It is known that impurities, such as Fe(III) and Al(III), form soluble oxalate complexes in water, enhancing the purity of the REE products [13,48]. However, the main disadvantages of precipitation stripping using oxalic acid are the high cost and the environmental issues related to the use of oxalic acid. Therefore, when only limited amounts of impurities are present in REE solutions, the use of ammonium or sodium hydrogen carbonate instead of oxalic acid is recommended [13]. The precipitate was recovered by filtration, followed by washing with 500 mL of ethanol and 1000 mL of distilled water. The precipitate was dried in an oven at $110 \text{ }^\circ\text{C}$ for 60 min, after which it was calcined in a muffle furnace at $900 \text{ }^\circ\text{C}$ for 1.5 h. The resulting rare-earth oxide (REO) product was analysed by XRD (Figure S9), which only showed the presence of the most concentrated REO, i.e. Yb_2O_3 for SX3 and Y_2O_3 for SX5 and SX6, with the peaks of the different other REE overlapping. Elemental analysis was conducted on solutions containing 100 mg of each REO concentrate, dissolved into 50 mL of 2 wt% HNO_3 . The relative purity of the Tm-group elements (Tm, Yb, Lu, after SX3) was 99.8%, while the purity of Er (after SX5) was only 8% (Y content was 85.5 wt%), and the purity of the Dy-group elements (Dy, Ho, Y, after SX6) was 98.7%.

4. Conclusions

This paper investigated a non-aqueous solvent extraction process using ethylene glycol in the more polar phase (+10 vol% water) and Cyanex 923 as extractant, for the separation of a group of HREEs (Dy,

Ho, Er, Tm, Yb, Lu and Y). This process can be plugged into an existing hydrometallurgical flowsheet, as it comprises the dissolution of an REE concentrate in ethylene glycol, in the presence of hydrochloric acid. Based on batch experiments, a conceptual flowsheet was developed and tested for its feasibility in lab-scale mixer-settlers, and then expanded and adjusted as a result of optimization during these mixer-settlers experiments. It showed that the HREEs can be separated successfully into 2 groups: a Dy-group containing Dy, Ho, Er and Y, and a Tm-group containing Tm, Yb and Lu. The purity of both groups in the original feed solution was 57% and 34%, respectively. The purity of the group-separated REEs after precipitation and calcination was 99.8% for the Dy-group and 98.7% for the Tm-group indicating successful group-separation, using only 16 stages of mixer-settlers. It was attempted to further purify Er from the Dy-group elements using an extra 4 stages of extraction and 3 stages of scrubbing, but it turned out that further optimization is necessary to improve the product purity. Overall, this non-aqueous solvent extraction process developed for HREE separation uses only a limited number of stages, while conventional processes are using more than three times as many stages and consume large amounts of acids and bases for pH control and stripping to achieve the same degree of separation. Future research should focus on closing the loops within the process, further improving the solvent extraction parameters for separation and purification of single REEs and full industrial integration and implementation.

CRediT authorship contribution statement

Brecht Dewulf: Conceptualization, Investigation, Writing – original draft. **Sofía Riaño:** Investigation, Writing – review & editing. **Koen Binnemans:** Conceptualization, Supervision, Writing – review & editing, Funding acquisition.

Declaration of Competing Interest

The authors declare that they have no known competing financial interests or personal relationships that could have appeared to influence the work reported in this paper.

Acknowledgements

The research leading to this manuscript received funding from the European Union's EU Framework Programme for Research and Innovation Horizon 2020 under grant agreement no. 776846 (NEMO).

Appendix A. Supplementary material

The following contents are presented in the Supporting Information file, free of charge: used ICP-OES lines (Table S1), description of the analysis of rare-earth hydroxide concentrate, explanation on preparation of synthetic rare-earth hydroxide concentrate, table of composition industrial and synthetic rare-earth hydroxide concentrate (Table S2–3), picture of leaching reactor (Figure S1), explanation on preparation of ethylene glycol feed solutions, picture of mixer-settler mini-pilot (Figure S2), summary of mixer-settler operating conditions (Table S4), effect of temperature on dissolution rate of $\text{RE}(\text{OH})_3$ (Figure S3), effect of water and LiCl concentration on extraction of impurities (Figure S4), effect of Cyanex 923 concentration on extraction of impurities (Figure S5), separation factors of the optimised NASX system (Table S5), McCabe-Thiele diagram for Fe and Zn extraction, Tm extraction, Er scrubbing, Er extraction, Y scrubbing, Dy and Y extraction (Figure S6), table with extraction results after SX1–6 (Table S6), REE concentration profile for SX4 and SX 5 (Figure S7–8), stripping results for LP obtained after SX3, 5 and 6 (Table S7), XRD diffractogram REO obtained from SX3, SX5 and SX6 LP phases after stripping and calcination. Supplementary data to this article can be found online at <https://doi.org/10.1016/j.seppur.2022.120882>.

References

- [1] T. Liu, J.i. Chen, Extraction and separation of heavy rare earth elements: a review, *Sep. Purif. Technol.* 276 (2021) 119263, <https://doi.org/10.1016/j.seppur.2021.119263>.
- [2] K. Binnemans, P. McGuinness, P.T. Jones, Rare-earth recycling needs market intervention, *Nat. Rev. Mater.* 6 (6) (2021) 459–461, <https://doi.org/10.1038/s41578-021-00308-w>.
- [3] K. Binnemans, P.T. Jones, B. Blanpain, T. Van Gerven, Y. Yang, A. Walton, M. Buchert, Recycling of rare earths: a critical review, *J. Clean. Prod.* 51 (2013) 1–22, <https://doi.org/10.1016/j.jclepro.2012.12.037>.
- [4] S.M. Jowitz, T.T. Werner, Z. Weng, G.M. Mudd, Recycling of the rare earth elements, *Curr. Opin. Green Sustain. Chem.* 13 (2018) 1–7, <https://doi.org/10.1016/j.cogsc.2018.02.008>.
- [5] K. Binnemans, P.T. Jones, T. Müller, L. Yurramendi, Rare earths and the balance problem: how to deal with changing markets? *J. Sustain. Metall.* 4 (1) (2018) 126–146, <https://doi.org/10.1007/s40831-018-0162-8>.
- [6] K. Binnemans, P.T. Jones, B. Blanpain, T. Van Gerven, Y. Pontikes, Towards zero-waste valorisation of rare-earth-containing industrial process residues: a critical review, *J. Clean. Prod.* 99 (2015) 17–38, <https://doi.org/10.1016/j.jclepro.2015.02.089>.
- [7] Z.H. Wang, G.X. Ma, J. Lu, W.P. Liao, D.Q. Li, Separation of heavy rare earth elements with extraction resin containing 1-hexyl-4-ethylolyl isopropylphosphonic acid, *Hydrometallurgy*. 66 (1-3) (2002) 95–99, [https://doi.org/10.1016/S0304-386X\(02\)00109-3](https://doi.org/10.1016/S0304-386X(02)00109-3).
- [8] Z. Wang, G. Ma, D. Li, Extraction and separation of heavy rare earth(III) with extraction resin containing di(2,4,4-trimethyl pentyl) phosphonic acid (cyanex 272), *Solvent Extr. Ion Exch.* 16 (3) (1998) 813–828, <https://doi.org/10.1080/07366299808934554>.
- [9] L.i. Chen, J.i. Chen, Asymmetric membrane containing ionic liquid [A336][P507] for the preconcentration and separation of heavy rare earth lutetium, *ACS Sustain. Chem. Eng.* 4 (5) (2016) 2644–2650, <https://doi.org/10.1021/acsschemeng.6b00141>.
- [10] Y. Wang, L.i. Chen, Y. Yan, J.i. Chen, J. Dai, X. Dai, Separation of adjacent heavy rare earth Lutetium (III) and Ytterbium (III) by task-specific ionic liquid Cyphos IL 104 embedded polymer inclusion membrane, *J. Memb. Sci.* 610 (2020) 118263, <https://doi.org/10.1016/j.memsci.2020.118263>.
- [11] Y. Liu, H.S. Jeon, M.S. Lee, Solvent extraction of Pr and Nd from chloride solution by the mixtures of Cyanex 272 and amine extractants, *Hydrometallurgy* 150 (2014) 61–67, <https://doi.org/10.1016/j.hydromet.2014.09.015>.
- [12] F. Xie, T.A. Zhang, D. Dreisinger, F. Doyle, A critical review on solvent extraction of rare earths from aqueous solutions, *Miner. Eng.* 56 (2014) 10–28, <https://doi.org/10.1016/j.mineng.2013.10.021>.
- [13] D. Qi, *Hydrometallurgy of Rare Earths: Extraction and Separation*, Elsevier, Amsterdam, 2018.
- [14] J. Zhang, B. Zhao, B. Schreiner, Separation hydrometallurgy of rare earth elements, Springer International Publishing, Basel (2016), <https://doi.org/10.1007/978-3-319-28235-0>.
- [15] L. Shen, J. Chen, L. Chen, C. Liu, D. Zhang, Y. Zhang, W. Su, Y. Deng, Extraction of mid-heavy rare earth metal ions from sulphuric acid media by ionic liquid [A336][P507], *Hydrometallurgy* 161 (2016) 152–159, <https://doi.org/10.1016/j.hydromet.2016.01.015>.
- [16] E. Anticó, A. Masana, M. Hidalgo, V. Salvadó, M. Iglesias, M. Valiente, Solvent extraction of yttrium from chloride media by di(2-ethylhexyl)phosphoric acid in kerosene. speciation studies and gel formation, *Anal. Chim. Acta* 327 (3) (1996) 267–276, [https://doi.org/10.1016/0003-2670\(96\)00103-1](https://doi.org/10.1016/0003-2670(96)00103-1).
- [17] L. Chen, J. Chen, Y. Jing, D. Li, Comprehensive appraisal and application of novel extraction system for heavy rare earth separation on the basis of coordination equilibrium effect, *Hydrometallurgy* 165 (2016) 351–357, <https://doi.org/10.1016/j.hydromet.2015.12.007>.
- [18] X. Wang, W. Li, W. Wang, S. Meng, D. Li, Influence of isoctanol on the interfacial activity and mass transfer of ytterbium(III) using 2-ethylhexylphosphonic acid mono-2-ethylhexyl ester as an acidic extractant, *J. Chem. Technol. Biotechnol.* 84 (2) (2009) 269–274, <https://doi.org/10.1002/jctb.2034>.
- [19] F.X. Cheng, S. Wu, Y. Liu, S.L. Wang, B. Zhang, C.S. Liao, C.H. Yan, Minimum amount of extracting solvent for AB/BC countercurrent separation using aqueous feed, *Sep. Purif. Technol.* 131 (2014) 8–13, <https://doi.org/10.1016/j.seppur.2014.04.031>.
- [20] C. Liao, S. Wu, F. Cheng, S. Wang, Y. Liu, B.o. Zhang, C. Yan, Clean separation technologies of rare earth resources in China, *J. Rare Earths*. 31 (4) (2013) 331–336, [https://doi.org/10.1016/S1002-0721\(12\)60281-6](https://doi.org/10.1016/S1002-0721(12)60281-6).
- [21] V.V. Belova, Development of solvent extraction methods for recovering rare earth metals, *Theor. Found. Chem. Eng.* 51 (4) (2017) 599–609, <https://doi.org/10.1134/S004057951605002X>.
- [22] M.K. Jha, A. Kumari, R. Panda, J. Rajesh Kumar, K. Yoo, J.Y. Lee, Review on hydrometallurgical recovery of rare earth metals, *Hydrometallurgy* 161 (2016) 77–101, <https://doi.org/10.1016/j.hydromet.2016.01.035>.
- [23] K. Binnemans, P.T. Jones, Solvometallurgy: an emerging branch of extractive metallurgy, *J. Sustain. Metall.* 3 (3) (2017) 570–600, <https://doi.org/10.1007/s40831-017-0128-2>.
- [24] Z. Li, B. Dewulf, K. Binnemans, Nonaqueous solvent extraction for enhanced metal separations: concept, systems, and mechanisms, *Ind. Eng. Chem. Res.* 60 (48) (2021) 17285–17302, <https://doi.org/10.1021/acs.iecr.1c02287>.
- [25] N.K. Batchu, T. Vander Hoogerstraete, D. Banerjee, K. Binnemans, Non-aqueous solvent extraction of rare-earth nitrates from ethylene glycol to *n*-dodecane by Cyanex 923, *Sep. Purif. Technol.* 174 (2017) 544–553, <https://doi.org/10.1016/j.seppur.2016.10.039>.
- [26] N.K. Batchu, T. Vander Hoogerstraete, D. Banerjee, K. Binnemans, Separation of rare-earth ions from ethylene glycol (+LiCl) solutions by non-aqueous solvent extraction with Cyanex 923, *RSC Adv.* 7 (72) (2017) 45351–45362, <https://doi.org/10.1039/C7RA09144C>.
- [27] N.K. Batchu, B. Dewulf, S. Riaño, K. Binnemans, Development of a solvometallurgical process for the separation of yttrium and europium by Cyanex 923 from ethylene glycol solutions, *Sep. Purif. Technol.* 235 (2020) 116193, <https://doi.org/10.1016/j.seppur.2019.116193>.
- [28] B. Dewulf, N.K. Batchu, K. Binnemans, Enhanced separation of neodymium and dysprosium by nonaqueous solvent extraction from a polyethylene glycol 200 phase using the neutral extractant cyanex 923, *ACS Sustain. Chem. Eng.* 8 (51) (2020) 19032–19039, <https://doi.org/10.1021/acsschemeng.0c07207>.
- [29] Z. Li, X. Li, S. Raiguel, K. Binnemans, Separation of transition metals from rare earths by non-aqueous solvent extraction from ethylene glycol solutions using Aliquat 336, *Sep. Purif. Technol.* 201 (2018) 318–326, <https://doi.org/10.1016/j.seppur.2018.03.022>.
- [30] M. Orefice, H. Audoor, Z. Li, K. Binnemans, Solvometallurgical route for the recovery of Sm Co, Cu and Fe from SmCo permanent magnets, *Sep. Purif. Technol.* 219 (2019) 281–289, <https://doi.org/10.1016/j.seppur.2019.03.029>.
- [31] C. Deferm, B. Onghena, V.T. Nguyen, D. Banerjee, J. Franssaer, K. Binnemans, Non-aqueous solvent extraction of indium from an ethylene glycol feed solution by the ionic liquid Cyphos IL 101: speciation study and continuous counter-current process in mixer-settlers, *RSC Adv.* 10 (41) (2020) 24595–24612.
- [32] EU Research and Innovation EU Horizon 2020, Near-zero-waste recycling of low-grade sulphidic mining waste for critical-metal, mineral and construction raw-material production in a circular economy (NEMO), (2018). <https://h2020-nemo.eu/> (accessed December 16, 2021).
- [33] F.J. Alguacil, F.A. López, The extraction of mineral acids by the phosphine oxide Cyanex 923, *Hydrometallurgy* 42 (2) (1996) 245–255, [https://doi.org/10.1016/0304-386X\(95\)00101-L](https://doi.org/10.1016/0304-386X(95)00101-L).
- [34] M. Orefice, V.T. Nguyen, S. Raiguel, P.T. Jones, K. Binnemans, Solvometallurgical process for the recovery of tungsten from scheelite, *Ind. Eng. Chem. Res.* 61 (1) (2022) 754–764, <https://doi.org/10.1021/acs.iecr.1c03872>.
- [35] IUPAC, Solubility data series volume 22: scandium, yttrium, lanthanum and lanthanide halides in nonaqueous solvents, Pergamon Press, Oxford, 1985.
- [36] E. Dziwinski, J. Szymanowski, Composition of CYANEX® 923, CYANEX® 925, CYANEX® 921 and TOPO, *Solvent Extr. Ion Exch.* 16 (6) (1998) 1515–1525, <https://doi.org/10.1080/07366299808934592>.
- [37] E.D. Doidge, I. Carson, J.B. Love, C.A. Morrison, P.A. Tasker, The influence of the Hofmeister bias and the stability and speciation of chloridolanthanates on their extraction from chloride media, *Solvent Extr. Ion Exch.* 34 (7) (2016) 579–593, <https://doi.org/10.1080/07366299.2016.1245051>.
- [38] Z. Hagiwara, A. Banno, A. Kamei, The Er-Tm separation factor in the presence of chelating agent and elution behavior of binary mixtures of Er and Tm, *J. Inorg. Nucl. Chem.* 31 (10) (1969) 3295–3301, [https://doi.org/10.1016/0022-1902\(69\)80116-8](https://doi.org/10.1016/0022-1902(69)80116-8).
- [39] Y. Han, J.i. Chen, Y. Deng, T. Liu, H. Li, D. Li, An innovative technique for the separation of ion-adsorption high yttrium rare earth ore by Er (III) / Tm (III) grouping first, *Sep. Purif. Technol.* 280 (2022) 119929, <https://doi.org/10.1016/j.seppur.2021.119929>.
- [40] L.i. Chen, H. Li, J.i. Chen, D. Li, T. Liu, Separation of heavy rare earths by di-(2-ethylhexyl) phosphonic acid: from fundamentals to cascade extraction simulation, *Miner. Eng.* 149 (2020) 106232, <https://doi.org/10.1016/j.mineng.2020.106232>.
- [41] T. Sato, Liquid-liquid extraction of rare-earth elements from aqueous acid solutions by acid organophosphorus compounds, *Hydrometallurgy* 22 (1-2) (1989) 121–140, [https://doi.org/10.1016/0304-386X\(89\)9045-5](https://doi.org/10.1016/0304-386X(89)9045-5).
- [42] R.A. Leonard, Design rules for solvent extraction, *Solvent Extr. Ion Exch.* 17 (3) (1999) 597–612, <https://doi.org/10.1080/07366299908934629>.
- [43] F.R. Chen, H.F. Chen, Pervaporation separation of ethylene glycol-water mixtures using crosslinked PVA-PES composite membranes. part I. effects of membrane preparation conditions on pervaporation performances, *J. Memb. Sci.* 109 (2) (1996) 247–256, [https://doi.org/10.1016/0376-7388\(95\)00195-6](https://doi.org/10.1016/0376-7388(95)00195-6).
- [44] X. Feng, R.Y.M. Huang, Pervaporation with chitosan membranes. I. Separation of water from ethylene glycol by a chitosan/polysulfone composite membrane, *J. Memb. Sci.* 116 (1996) 67–76, [https://doi.org/10.1016/0376-7388\(96\)00022-1](https://doi.org/10.1016/0376-7388(96)00022-1).
- [45] R. Guo, C. Hu, B. Li, Z. Jiang, Pervaporation separation of ethylene glycol/water mixtures through surface crosslinked PVA membranes: coupling effect and separation performance analysis, *J. Memb. Sci.* 289 (1-2) (2007) 191–198, <https://doi.org/10.1016/j.memsci.2006.11.055>.
- [46] M.K. Sinha, S. Pramanik, S.K. Sahu, L.B. Prasad, M.K. Jha, B.D. Pandey, Development of an efficient process for the recovery of zinc and iron as value added products from the waste chloride solution, *Sep. Purif. Technol.* 167 (2016) 37–44, <https://doi.org/10.1016/j.seppur.2016.04.049>.
- [47] A. Verma, R. Kore, D.R. Corbin, M.B. Shiflett, Metal recovery using oxalate chemistry: a technical review, *Ind. Eng. Chem. Res.* 58 (34) (2019) 15381–15393, <https://doi.org/10.1021/acs.iecr.9b02598>.
- [48] M.S. Archambo, S.K. Kawatra, Extraction of rare earths from red mud iron nugget slags with oxalic acid precipitation, *Miner. Process. Extr. Metall. Rev.* 43 (2021) 1–8, <https://doi.org/10.1080/08827508.2021.1927729>.